Study of antineutrinos from the Earth and the Cosmos with the Borexino detector

Sandra Zavatarelli*, M. Agostini, K. Altenmuller, S. Appel, V. Atroshchenko, Z. Bagdasarian, D. Basilico, G. Bellini,J. Benziger, R. Biondi, D. Bravo, B. Caccianiga, A. Caminata, F. Calaprice, P. Cavalcante, A. Chepurnov, D. D'Angelo, S. Davini, A. Derbin, A. Di Giacinto, V. Di Marcello, X.F. Ding, A. Di Ludovico, L. Di Noto, I. Drachnev, A. Formozov, D. Franco, C. Galbiati, C. Ghiano, M. Giammarchi, A. Goretti, A.S. Gottel, M. Gromov, D. Guffanti, Aldo Ianni, Andrea Ianni, A. Jany, D. Jeschke, V. Kobychev, G. Korga, S. Kumaran, M. Laubenstein, E. Litvinovich, P. Lombardi, I. Lomskaya, L. Ludhova, G. Lukyanchenko, L. Lukyanchenko, I. Machulin, J. Martyn, E. Meroni, M. Meyer, L. Miramonti, M. Misiaszek, V. Muratova, B. Neumair, M. Nieslony, R. Nugmanov, L. Oberauer, V. Orekhov, F. Ortica, M. Pallavicini, L. Papp, L. Pelicci, O Penek, L. Pietrofaccia, N. Pilipenko, A. Pocar, G. Raikov, M.T. Ranalli, G. Ranucci, A. Razeto, A. Re, M. Redchuk, A. Romani, N. Rossi, S. Schonert, D. Semenov, G. Settanta, M. Skorokhvatov, A. Singhal, O. Smirnov, A. Sotnikov, Y. Suvorov, R. Tartaglia, G. Testera, J. Thurn, E. Unzhakov, F. Villante, A. Vishneva, R.B. Vogelaar, F. von Feilitzsch, M. Wojcik, M. Wurm, S. Zavatarelli, K. Zuber, and G. Zuzel (Borexino Collaboration)

**Istituto Nazionale di Fisica Nucleare - Sezione di Genova, Via Dodecaneso 33, 16146 Genoa, Italy*
E-mail: sandra.zavatarelli@ge.infn.it

The largest amount of antineutrinos detected about the Earth is emitted by the natural radioactive decays of ^{232}Th and ^{238}U chains isotopes and of ^{40}K. Other flux components are yielded by cosmic rays interactions in the atmosphere or by possible extra-terrestrial sources such as supernovae explosions, gamma ray bursts, GW events and solar flares. This contribution is aimed to summarise the results obtained by the Borexino experiment about antineutrinos from the Earth and from extraterrestrial sources.

Keywords: Antineutrinos; Geonetrinos; solar flares; diffuse supernovae background.

1. Introduction

Large underground ultrapure liquid scintillators are very suitable to antineutrinos studies. Low energy neutrinos such as solar neutrinos are in general detected through the elastic scattering process on electrons but for electron antineutrinos a specific interaction channel can be exploited, the Inverse Beta-Decay (IBD) mechanism on the free proton:

$$\bar{\nu}_e + p \rightarrow n + e^+ \tag{1}$$

The emitted positron deposits its kinetic energy and annihilates almost immediately, inducing a prompt signal whose visible energy E_{prompt} is directly correlated with the incident antineutrino energy $E_{\bar{\nu}_e}$:

$$E_{prompt} = E_{\bar{\nu}_e} - 0.784\,\mathrm{MeV}. \tag{2}$$

The neutron thermalizes and is captured by a proton with the mean capture time: $\sim \tau = 254.5 \pm 1.8 \mu$s.[1] The IBD cross section is on average a factor ~ 100 higher than elastic scattering at few MeV. Moreover the fast time coincidence between the positron annihilation and the neutron capture provides an almost background free signature, that allows to investigate also tiny flux components. By exploiting this detection mechanism, Borexino[2] has robustly detected the geo-neutrino signal and begun to place constraints on the amount of radiogenic heating in the Earth's interior: the null-hypothesis of observing a geoneutrino signal from the mantle has been excluded at a 99.0% C.L. and the overall production of radiogenic heat constrained to $38.2\ ^{+13.6}_{-12.7}$ TW.[3] The extreme radiopurity of the Borexino detector has also allowed to set new limits on diffuse supernova antineutrino background for in the previously unexplored energy region below 8 MeV,[4] and to obtain the best upper limits on all flavor antineutrino fluences in the few MeV energy range from solar flares,[4] gamma-ray bursts[5] and from gravitational wave events.[6] In the following sections we detail the analysis procedures and the results obtained by Borexino about geoneutrinos, diffuse supernovae background and possible time correlated signals with solar flares.

2. Geo-neutrinos

Geoneutrinos are electron antineutrinos ($\bar{\nu}_e$) emitted in the β decays of long-lived isotopes, which are present in the Earth, such as ^{40}K and the ^{238}U and ^{232}Th chain unstable isotopes.[11] The decay schemes and the released heat are summarised in the following equations:

$$^{238}\mathrm{U} \rightarrow ^{206}\mathrm{Pb} + 8\alpha + 8e^- + 6\bar{\nu}_e + 51.7 \quad \mathrm{MeV} \tag{3}$$

$$^{235}\mathrm{U} \rightarrow ^{207}\mathrm{Pb} + 7\alpha + 4e^- + 4\bar{\nu}_e + 46.4\ \mathrm{MeV} \tag{4}$$

$$^{232}\mathrm{Th} \rightarrow ^{208}\mathrm{Pb} + 6\alpha + 4e^- + 4\bar{\nu}_e + 42.7\ \mathrm{MeV} \tag{5}$$

$$^{40}\mathrm{K} \rightarrow ^{40}\mathrm{Ca} + e^- + \bar{\nu}_e + 1.31\ \mathrm{MeV}\ (89.3\%) \tag{6}$$

$$^{40}\mathrm{K} + \mathrm{e} \rightarrow ^{40}\mathrm{Ar} + \nu_e + 1.505\ \mathrm{MeV} \quad (10.7\%) \tag{7}$$

Since the present-day isotopic abundance of ^{235}U is small (0.7%), the overall contribution of ^{238}U, ^{232}Th, and ^{40}K is largely predominant. Information about the deep Earth's composition is mainly based on indirect probes: seismologic data constrains the density profile, while geochemistry provides predictions based on chemical compositions of upper Earth's rocks, chondritic meteorites, and the Sun photosphere. The surface of the Earth is emitting an heat flow at an estimated rate of 47 ± 2 TW.[12] This result is based on $\sim$ 40,000 observations of heat conduction in surface rocks and corrected for hydrothermal circulation and volcanism. Measurements of Th, U and K in the continental crust rocks prove that at least $\sim$8 TW of this heat

is from radiogenic decays but is not at all known what proportion of the overall surface heat flow comes from radioactive decays and how much is from primordial sources such as the gravitational energy released after core formation or the kinetic energy of accretion bombardment.

Geo-neutrinos give us a way of measuring the amount of this radiogenic heat directly: the heat released is in a well fixed ratio with the total mass of Heat Producing Elements (HPE's) inside the Earth. Thus, it is possible to extract from the measured geo-neutrino fluxes several geological information unreachable by other means. The idea of studying geo-neutrinos dates back to the sixties[7,8] but only in 1998 it was proposed the idea of using solar neutrino and reactor neutrino detectors[9,10]: presently, two large-volume, liquid-scintillator neutrino experiments, KamLAND in Japan[13–15] and Borexino in Italy,[3,16–18] have been able to measure the geo-neutrino signal. The typical fluxes are of the order of 10^6 cm^{-2}s^{-1} and with cross section values of 10^{-43} cm^{-2} only a hand-full number of interactions, few tens per year are expected with the current-size detectors. This means, underground laboratories are crucial to shield the detector from cosmic radiation and make possible their measurement. Since the inverse beta decay (IBD) on protons has a threshold of 1.8 MeV (Eq. 1) and both the ^{40}K and ^{235}U geo-neutrinos spectra are below (Fig. 1), they cannot be detected by this process. However, the elemental abundances ratios are much better known than the absolute abundances. Therefore, by measuring the absolute content of ^{238}U and ^{232}Th, also the overall amount of ^{40}K and ^{235}U can be inferred with an improved precision.

Geo-neutrino spectrum extends up to 3.26 MeV and the ^{238}U and ^{232}Th contributions can be distinguished according to their different end-points (Fig. 1).

The most recent Borexino analysis is based on 3263 days of data taking in the period December 2007 - April 2019.

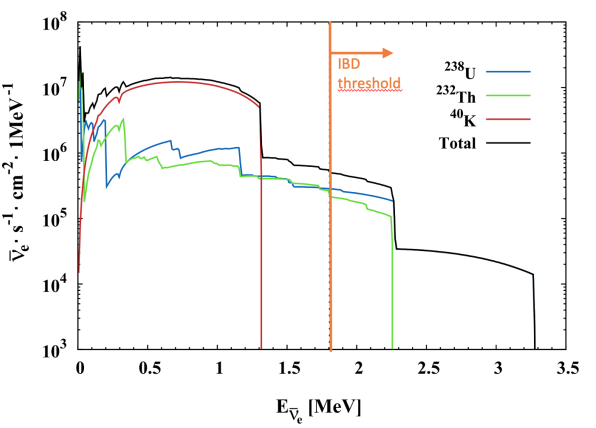

Fig. 1. Geoneutrino fluxes[3] from different isotopes and the overall signal at LNGS calculated with geophysical and geochemical inputs from[24] for the far-field lithosphere and from[23] for the local crust.

To select the $\bar{\nu}_e$ candidates we apply the following criteria: we discard events occurring within 2 ms of every muon crossing the outer detector to reject cosmogenic neutrons. In case of muons crossing the inner detector long-lived cosmogenic nuclides such a ^{9}Li may be produced: to reduce this possible background a different veto ranging from 0.2 to 2 s is applied after the muon depending on the deposited energy, the track reconstruction quality and the eventually associated neutrons. Independently from a detected muon, we ask that selected events are neither preceded or followed by neutron-like events within a 2 ms window. The coincidences are searched for at a distance between the reconstructed positions Δr < 1.3 m, that accounts for the uncertainty of the spatial reconstruction algorithm and the free path of the 2.2 MeV γ's and with Δt in the range 20–1280 μs ($\sim$5 neutron capture time) for single events, and 2.5–12.5 μs for double cluster events. We remind that if a decay triggering the Borexino DAQ is followed within 16.5 μs by other decays, it is classified as a unique event with multiple clusters. To reduce the external γ background from radioactive decays in the detector materials, we accept only candidates having the prompt event position reconstructed inside the inner detector at distance larger than 10 cm with respect to the the time-varying IV surface: $D_{IV,prompt} > 10\,cm$. The energy of the prompt event is required to be above the value corresponding to the IBD threshold, considering the energy resolution ($N_{p.e.,prompt} > 408$ p.e.), while for the delayed event, the energy cut was tuned to cover the gamma peak from neutron capture on proton and on carbon ($700 < N_{p.e.,delayed} < 3000$ p.e.). The lower limit is justified because photons at the edge of the scintillator can escape, depositing only a fraction of their total energy. This limit was increased to 860 p.e. during the detector purifications in 2010-2011 to remove the time-correlated $\beta + (\alpha + \gamma)$ decays of ^{214}Bi-^{214}Po, having a time constant close to the neutron capture time. Such background was relevant only during the purifications as a consequence of the increased radon contamination. Finally a pulse shape $\alpha - \beta$ discrimination is applied based on a trained MultiLayerPerceptron binary classifier [3] : $\mathrm{MLP}_D > 0.8$ for delayed signals.

The combined efficiency of the cuts is determined by Monte Carlo to be (85$\pm$1.0)%. The total efficiency-corrected exposure for the data set is (1.29 $\pm$ 0.05) $\times$ 10^{32} protons $\times$ year with an increase by a factor of two over the previous Borexino analysis reported in 2015. We have identified 154 candidates passing all the selection cuts. The estimated background, that mimics $\bar{\nu}_e$ candidates, amounts to 8.28 $\pm$ 1.01 events, mainly due to random coincidences, residual ^{9}Li decays and ^{13}C(α,n)^{16}O reactions in the scintillator.

Antineutrinos from nuclear reactor power plants are the main background to the geo-neutrino measurements. The $\bar{\nu}_e$ flux comes primarily from the beta decays of neutron-rich fragments produced in the fission of four isotopes: ^{235}U, ^{238}U, ^{239}Pu, and ^{241}Pu. The expected fluxes can be estimated from the knowledge of the monthly energy production at each reactor site, including the neutrino propagation effects. At present, there are about 440 nuclear power reactors in the world, providing,

nominally, a total amount of about 1200 Thermal GW, corresponding to about 400 Electrical GW. Since there are no nuclear power plants close by, the Gran Sasso laboratory is well suited for geo-neutrino studies. According to a detailed computation[22] based on the information retrieved by the International Atomic Energy Agency database[19] we expect 91-98 events in our sample whereas the main source of uncertainty in the prediction comes from the knowledge of the energy spectrum for each fuel component at the source. The lowest value (91.9 ± 1.6) is obtained when the spectra are normalised to the measurements of reactor neutrino experiments[20,21] and they include also the so called "5 MeV excess".

A smaller background can also be induced by atmospheric neutrinos. Because of the uncertainty of the relevant fluxes and cross sections, this contribution is poorly constrained: we have estimated 9.2 ± 4.6 event in our sample.

Both reactor and atmospheric $\bar{\nu}_e$ are more energetic respect to the geo-neutrino; therefore they can be experimentally disentangled thanks to a fit of prompt event energies. An unbinned likelihood fit of the energy spectrum of selected prompt events has been performed.

In Fig. 2 the selected candidates and the fit results are shown. Using the value ratio for the masses of Th and U, m(Th)/m(U)=3.9, suggested by the chondritic metheorithes, our best fit yield $N_{geo} = 52.6^{+9.4}_{-8.6}(stat)^{+2.7}_{-2.1}(sys)$ events, with 18% precision. A compatible result was found when contributions from ^{238}U and ^{232}Th were both fit as free parameters. Antineutrino background from reactors is fit unconstrained and found compatible with the expectations. The measured geo-neutrino signal corresponds to fluxes at the detector from decays in the U and Th chains of $\Phi_U = 2.8^{+0.6}_{-0.4} \cdot 10^6$ cm^{-2}s^{-1} and $\Phi_{Th} = 2.6^{+0.6}_{-0.4} \cdot 10^6$ cm^{-2}s^{-1} respectively.

To connect the number of geo-neutrinos detected by an experiment with the overall radioactivity in the crust and in the mantle, we have to rely on our knowledge

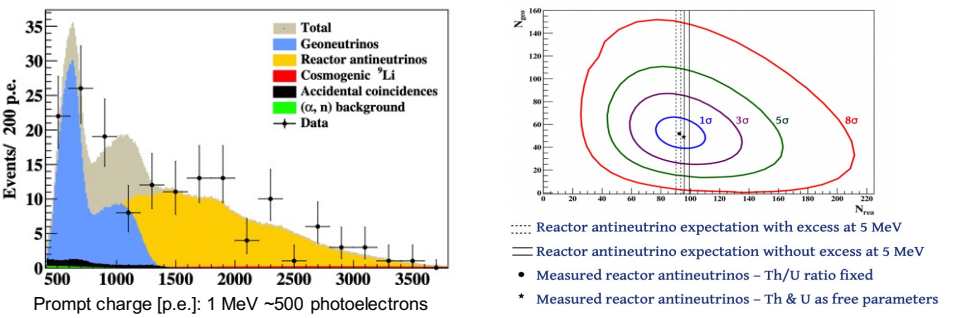

Fig. 2. **(Left)** Spectral fit of the data (black points assuming the chondritic Th/U ratio. Geoneutrinos (blue) and reactor antineutrinos (yellow) were kept as free fit parameters. Other non antineutrino backgrounds were constrained in the fit. **(Right)** The best fit point (black dot) and the 2D coverage contours for N_{geo} vs N_{rea}.

of the local geological conditions. Geoscientist developed models of the crust close to the Borexino site, based on geological surveys and on 3D models of all the layers up to the mantle boundary.[23,24] Both U and Th are lithophile i.e. "rock-loving" elements so they are believed to be concentrated in the crust and mantle and absent in the iron-made core. According to these studies 28.8 ± 5.6 events should have been induced by the crust radioactivity among the 154 candidates: we have therefore repeated the fit with separate contribution of mantle and crust geoneutrinos, the latter being constrained to the expectations within the error. A small difference in the relative amount of U and Th fraction in the two signals has been introduced according to geological predictions. The fit returns $N_{geo} = 23.7^{+10.7}_{-10.0}(stat)^{+1.2}_{-1.0}(sys)$ events: with a sensitivity study the null-hypothesis of observing geoneutrino signal from the mantle is excluded at a 99.0% C.L..

It is possible to extract from the measured geo-neutrino signal, the Earth's radiogenic heat power that is a fundamental question for understanding the plate tectonics and mantle convection. The uncertain distribution of HPE's in the deep Earth has to be included: two rather extreme cases are represented by the homogeneous mantle or by the assumption that all the U and Th are placed at the mantle core boundary. By following this conservative approach one can demonstrate that our measured mantle signal corresponds to the production of a radiogenic heat of 24.6 ± 11.1 TW (68% interval) from ^{238}U and ^{232}Th in the mantle. Assuming 18% contribution of ^{40}K in the mantle and 8.1 ± 1.9 TW of total radiogenic heat of the lithosphere, the Borexino estimate of the total radiogenic heat of the Earth is 38.2 $\pm$ 13.6 TW, which corresponds to $\sim$81% of the overall Earth's heat flux (47 TW). These values are compatible with different geological predictions, in the particular with the geodynamical BSE models,[25] however there is a $\sim 2.4\sigma$ tension with those Earth models which predict the lowest concentration of heat-producing elements in the mantle, such as cosmochemical ones.[25] In addition, by constraining the number of expected reactor antineutrino events, the existence of a hypothetical georeactor at the center of the Earth having power greater than 2.4 TW is excluded at 95% C.L..[26,27] In conclusion, Borexino confirms the feasibility of geoneutrino measurements as well as the validity of different geological models predicting the U and Th abundances in the Earth. This is an enormous success of both neutrino physics and geosciences. The next generation of large volume liquid scintillator detectors (such as JUNO and SNO+) has a strong potential to provide fundamental information about our planet and geoneutrinos may be the key tool to support the new discoveries about the deep Earth.

3. Diffuse supernovae neutrino background

The Diffuse Supernova Neutrino Background (DSNB) is formed by the stars that collapsed during the evolution of the Universe and it is made of neutrinos and antineutrinos of all flavours. The flux spectrum at the Earth can be parametrised

as[28]:

$$\frac{d\phi_\nu}{dE_\nu} = \frac{c}{H_0}\int_0^{z_{max}} \frac{dN_\nu(E'_\nu)}{dE'_\nu}\frac{R_{SN}(z)dz}{\sqrt{\Omega_m(1+z)^3+\Omega_\Lambda}}, \tag{8}$$

where c is the speed of light, z is the red shift, H_0 is Hubble constant, $R_{SN}(z)$ is the supernova rate at the distance z to the observer $\frac{dN_\nu(E'_\nu)}{dE'_\nu}$ is the neutrino emission spectrum for individual supernova, Ω_m and Ω_Λ are the relative densities of matter and dark energy in the Universe. The spectrum is sensitive to particular cosmological model through Ω_m and Ω_Λ and reflects the expansion of the Universe through the dependence on H_0.

The possible signal due to tiny, still undisclosed, extraterrestrial $\bar{\nu}_e$ fluxes, such as supernovae relic neutrinos, can be put in evidence as an excess of events with respect to the backgrounds and the known sources of $\bar{\nu}_e$. Borexino made a search for this possible signal, based on the data collected between December 2007–October 2017. The events selection is based on an approach similar to the one adopted in the geo-neutrino analysis, the only differences being more conservative muon and FV cuts. In detail we applied a veto of 2 s after each muon crossing the inner detector and we asked for a prompt event distance from the inner vessel larger than 25 cm: in the overall statistics we have selected 101 candidates.

As outlined in the previous sections, the most relevant sources of $\bar{\nu}_e$ events below 10 MeV are the Earth's radioactive isotopes and the nuclear reactors, while at higher energies the atmospheric neutrino background dominates the energy spectrum. Borexino made a comprehensive study of geo-neutrinos but the achieved precision, in particular on the mantle signal is still poor ($\sim 40\%$), With the aim to quote conservative limits, the minimal expected number of events for each background has been considered. For the geoneutrino signal we have therefore chosen the Minimal Radiogenic Earth model, which only includes the radioactivity from the crust and that, in our case, corresponds to 17.9 ± 2.1 events in our data sample.

The spectrum of reactor $\bar{\nu}_e$ is significant till $\sim$10 MeV. As discussed before, the flux calculation that includes the normalisation to reactor neutrino experiments data provides the lowest signal. We have taken this option being the most conservative: 61.1 ± 1.7 events among our candidates have been attributed to reactor $\bar{\nu}_e$. Finally the most serious background to the detection of DSNB fluxes at energies above 10 MeV is induced by the atmospheric neutrinos, i.e., the ν's and $\bar{\nu}$'s generated in the decay of secondary particles produced in the interactions of primary cosmic rays with Earth's atmosphere. After the simulation of detector response and by applying the same selection cuts as for real data, we have estimated 6.5 ± 3.2 IBD-like events in the present analysis statistics and in the equivalent $\bar{\nu}_e$ energy window 1.8–16.8 MeV. In the light of the large uncertainty on this background source, a conservative choice would be to not consider it at all in the upper limit calculations: this is the approach followed in Fig. 3. The model-independent limit for electron antineutrino

flux ($\Phi_{\bar{\nu}_e}$) in each energy bin (i) have been computed according to the equation:

$$\Phi_{\bar{\nu}_e,i} = \frac{N_{90,i}}{<\sigma>\cdot\varepsilon\cdot N_p\cdot T} \tag{9}$$

where N_{90} is the 90% C.L. upper limit for the number of antineutrino interactions obtained by following the Feldman-Cousins approach,[29] $<\sigma>$ is the mean cross-section of Inverse Beta Decay calculated according to[30] for each energy bin, ε=(0.850 $\pm$ 0.015) is the average detection efficiency, $N_p = (1.32 \pm 0.06) \times 10^{31}$ is the number of protons in the Borexino average fiducial volume mass and $T = 2485$ days is the total live-time. The other limits existing in literature are quoted on the same plot.

Borexino limits are the only existing below 8 MeV, thanks to the high energy resolution, the low intrinsic backgrounds, and the small reactor $\bar{\nu}_e$ flux at the Gran Sasso site.

4. Search for time correlated signals with solar flares

Solar flares are induced by the rearrangement of the solar magnetic field which also bring to the acceleration of charged particles. Pions, eventually produced in the flare's region by pp- and $p\alpha$-collisions, could then decay by emitting neutrinos with a mean neutrino energy expected around $\sim 10\,\mathrm{MeV}$.[35]

In the eighties R. Davis[36,37] advanced for the first time the possibility of neutrino emissions correlated with solar flares as an explanation for the excess of events in several runs of the Homestake Cl-Ar experiment. In general the production of $\bar{\nu}_e$ is expected to be smaller respect to ν_e due to the higher threshold of π^- generation in pp-collisions: for this reason we have searched for ν_x and $\bar{\nu}_x$ ($x = e, \mu, \tau$)

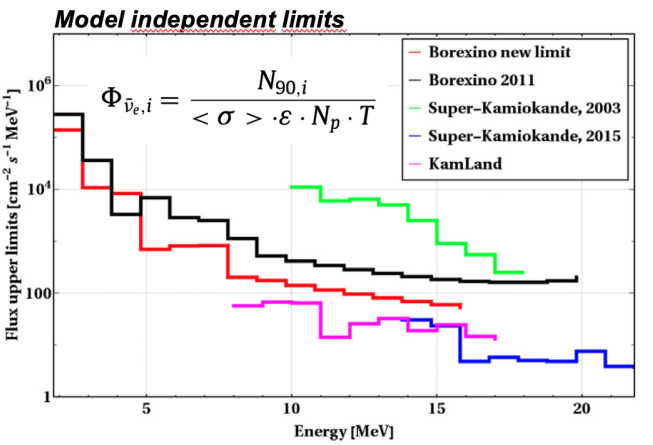

Fig. 3. Borexino model-independent limits on electron $\bar{\nu}_e$ fluxes from unknown sources compared with the results of other experiments (Super-Kamiokande,[31,32] KamLAND[33]) and older Borexino limits.[34]

signals correlated with solar flares by looking their elastic scattering on electrons in the Borexino scintillator. According to the assumption that the neutrino flux is proportional to the flare's intensity, we have only considered the most intense flares of M and X classes according to the GOES database.[38]

The analysis is based on the statistics collected between November 2009 and October 2017 : data acquired both by the primary and the FADC DAQ systems have been used in the energy interval of 1–15 MeV, while in the interval 0.25 – 1 MeV only the primary DAQ data have been considered. After removing muons and muon daughters, single events are selected without any fiducial volume cut in the interval of 1–15 MeV, while at lower energies a fiducial volume cut of 145 tons (75 cm from the IV) is applied to reduce the external radioactivity. In our study, an excess of single events above the measured background at the time of a flare is searched for. For the flare signal we choose a time window equal to the flare's duration according to the database, while the background is calculated in a time window of the same length but opened before the flare time. By requiring at least 95% of Borexino's up time for both windows we restrict our analysis to a 472 flares sample. No statistically significant excess of events is observed in correlation with the flares. The fluence limit for neutrinos of energy E_ν is calculated according to the equation:

$$\Phi_\nu(E_\nu) = \frac{N_{90}(E_\nu)}{N_e \sigma_{\text{eff}}(E_\nu)}, \tag{10}$$

where N_e is the number of electrons in the Borexino scintillator, that is, $N_e = 9.2 \cdot 10^{31}$ for the whole IV and $N_e = 4.8 \cdot 10^{31}$ for the 145 tons FV. The scattering of monoenergetic neutrinos with energy E_ν off electrons leads to recoil electrons with a Compton-like continuous energy spectrum with maximum energy $T_\nu^{max} = 2E_\nu^2/(m_e + 2E_\nu)$. For each neutrino energy bin, a corresponding recoiled electrons energy interval is computed by considering the cross section and the detector response function.

In order to set the fluence limits for flare-correlated neutrinos (antineutrinos) of electron and $(\mu + \tau)$ flavors individually, the corresponding cross section in Eq. 10 was set to σ_{ν_e} ($\sigma_{\bar{\nu}_e}$) and $\sigma_{\nu_{\mu,\tau}}$ ($\sigma_{\bar{\nu}_{\mu,\tau}}$), respectively. Figure 4 quotes Borexino limits obtained from the primary DAQ ($E_\nu < 3.5$ MeV) and the FADC DAQ ($E_\nu > 3.5$ MeV).

Limits for ν_e quoted by SNO[39] and an allowed band for the neutrino fluence that would have explained the Homestake run 117 excess of events are also shown for comparison.

As of today, Borexino sets the strongest limits on fluences of all neutrino flavors from the solar flares below 3–7 MeV. Under the hyphothesis that neutrino flux is proportional to the flare's intensity, Borexino's data excludes an intense solar flare occurred during run 117 of the Cl-Ar Homestake experiment as a possible source for the observed excess of events.

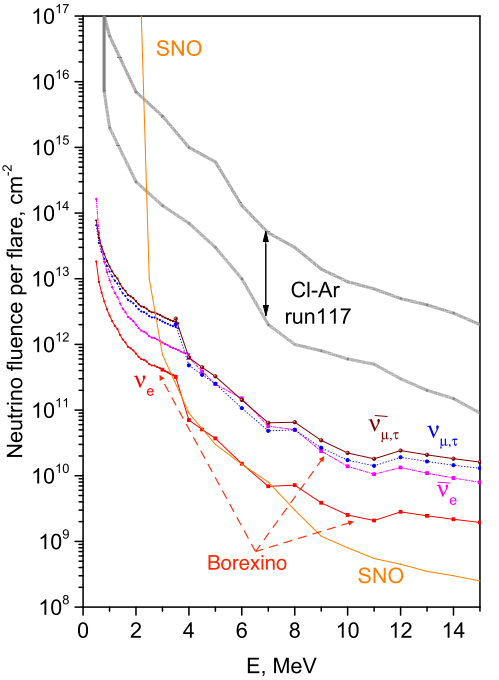

Fig. 4. Borexino 90% C.L. fluence upper limits obtained through elastic scattering for ν_e, $\bar{\nu}_e$, $\nu_{\mu,\tau}$, and $\bar{\nu}_{\mu,\tau}$. The limits by SNO[39] for ν_e are reported and the fluences that would have explained the Cl-Ar Homestake excess in run 117.

5. Conclusions

Large ultrapure liquid scintillators in underground laboratories have a strong potential for the comprehension of our planet energetics and in the various fields of experimental neutrino astronomy. Collecting more data in the incoming years with a network of detectors will be crucial to probe the very foundations of our understanding of the Universe and of our planet.

References

1. G. Bellini et al. (Borexino Collaboration), *J. Instrum.* **6**, P05005 (2011).
2. G. Alimonti et al. (Borexino Collaboration), *Nucl. Instr. and Meth. A* **600**, 58 (2009).
3. M. Agostini et al. (Borexino Collaboration), *Phys. Rev. D* **101**, 012009 (2020).
4. M. Agostini et al. (Borexino Collaboration), *Astropart. Phys.* **125**, 102509 (2021).
5. M. Agostini et al. (Borexino Collaboration), *Astropart. Phys.* **86**, 11 (2017).
6. M. Agostini et al. (Borexino Collaboration), *Ap. J.* **850**, 21 (2017).
7. G. Eder, *Nucl. Phys.* **78** (1966)
8. G. Marx, *Czech J. Phys. B* **19** (1969).
9. R. S. Raghavan et al., *Phys. Rev. Lett.* **80**, 635 (1998).
10. C. G. Rotschild, et al., *Geo. Res. Lett.* **25**, 1083 (1998).

11. G. Fiorentini, M. Lissia, and F. Mantovani, *Phys. Rep.* **453**, 117 (2007).
12. J. H. Davies and D. R. Davies, *Solid Earth* **1**, 5 (2010).
13. T. Araki et al. (KamLAND Collaboration), *Nature* **436**, 499 (2005).
14. S. Abe et al. (KamLAND Collaboration), *Phys. Rev. Lett.* **100**, 221803 (2008).
15. A. Gando et al. (KamLAND Collaboration), *Phys. Rev. D* **88**, 033001 (2013).
16. G. Bellini et al. (Borexino Collaboration), *Phys. Lett. B* **687**, 299 (2010).
17. G. Bellini et al. (Borexino Collaboration), *Phys. Lett. B* **722**, 295 (2013).
18. M. Agostini et al. (Borexino Collaboration), *Phys. Rev. D* **92**, 031101 (2015).
19. Nuclear Power Engineering Section, IAEA-PRIS database, http://www.iaea.org/pris/
20. F. P. An et al. (Daya Bay Collaboration), *Phys. Rev. Lett.* **116**, 061801 (2016).
21. F. P. An et al. (Daya Bay Collaboration), *Phys. Rev. Lett.* **118**, 099902(E) (2017).
22. M. Baldoncini, I. Callegari, G. Fiorentini, F. Mantovani, B. Ricci, V. Strati, and G. Xhixha, *Phys. Rev. D* **91**, 065002 (2015).
23. M. Coltorti et al., *Earth Planet. Sci. Lett.* **293**, 259 (2010).
24. Y. Huang, V. Chubakov, F. Manotavani, R. L. Rudnick, and W. F. McDonough, *Geochemistry, Geophysics, Geosystems* **14**, 2003 (2013).
25. O. Sramek, W. F. McDonough, E. S. Kite, V. Lekic, S. T. Dye, and S. Zhong, *Earth and Planet. Sci. Lett.* **361**, 356 (2013).
26. J. M. Herndon, *Proc. Natl. Acad. Sci. U.S.A. 93(2)*, 646 (1996).
27. J. M. Herndon and D. A. Edgerley, *arXiv:hep-ph/0501216.*
28. S. Ando and K. Sato, *New J. Phys* **6**, 170 (2004).
29. G. J. Feldman, R. D. Cousins, *Phys. Rev. D* **57**, 3873(1998).
30. A. Strumia, F. Vissani, *Phys. Lett. B* **564**, 42 (2003).
31. Y. Gando, et al. (Super-Kamiokande Collaboration), *Phys. Rev. Lett.* **90**, 171302 (2003).
32. H. Zhang, et al. (Super-Kamiokande Collaboration), *Astropart. Phys.* **60**, 41 (2015).
33. A. Gando, et al. (KamLAND Collaboration), *Astroph. J.* **745**, 193 (2012).
34. G. Bellini, et al. (Borexino Collaboration), *Phys. Lett. B* **696**, 191 (2011).
35. G. E. Kocharov, G. A. Kovaltsov, I. G. Usoskin, *Il nuovo cimento* **14 C**, 417 (1991).
36. R. Davis Jr., *Prog. Part. Nucl. Phys.* **32**, 13 (1994).
37. R. Davis Jr., *Nucl. Phys. Proc. Suppl.* **48**, 284 (1996).
38. GOES Database: https://hesperia.gsfc.nasa.gov/goes/goeseventlistings
39. B. Aharmim et al. (SNO Collaboration), *Astropart. Phys.* **551137**, 1 (2014).